OPEN ACCESS

University of BRISTOL

Publisher's PDF, also known as Version of record

Link to published version (if available):
10.1063/1.4879849

Link to publication record in Explore Bristol Research
PDF-document

University of Bristol - Explore Bristol Research
General rights

Diamond micro-Raman thermometers for accurate gate temperature measurements

Roland B. Simon, James W. Pomeroy, and Martin Kuball

Articles you may be interested in

Dynamic microscale temperature gradient in a gold nanorod solution measured by diffraction-limited nanothermometry
Appl. Phys. Lett. **107**, 121105 (2015); 10.1063/1.4931724

Single element Raman thermometry
Rev. Sci. Instrum. **84**, 064903 (2013); 10.1063/1.4810850

Current collapse in AlGaN/GaN transistors studied using time-resolved Raman thermography
Appl. Phys. Lett. **93**, 203510 (2008); 10.1063/1.3035855

Self-heating in a GaN based heterostructure field effect transistor: Ultraviolet and visible Raman measurements and simulations
J. Appl. Phys. **100**, 113718 (2006); 10.1063/1.2395681

Measurement of temperature distribution in multifinger AlGaN/GaN heterostructure field-effect transistors using micro-Raman spectroscopy
Appl. Phys. Lett. **82**, 124 (2003); 10.1063/1.1534935

Diamond micro-Raman thermometers for accurate gate temperature measurements

Roland B. Simon, James W. Pomeroy, and Martin Kuball
Center for Device Thermography and Reliability, H. H. Wills Physics Laboratory, University of Bristol, Tyndall Avenue, Bristol BS8 1TL, United Kingdom

Determining the peak channel temperature in AlGaN/GaN high electron mobility transistors and other devices with high accuracy is an important and challenging issue. A surface-sensitive thermometric technique is demonstrated, utilizing Raman thermography and diamond microparticles to measure the gate temperature. This technique enhances peak channel temperature estimation, especially when it is applied in combination with standard micro-Raman thermography. Its application to other metal-covered areas of devices, such as field plates is demonstrated. Furthermore, this technique can be readily applied to other material/device systems. © 2014 AIP Publishing LLC. [http://dx.doi.org/10.1063/1.4879849]

Channel temperature is a key device parameter, impacting both the performance and reliability of AlGaN/GaN high electron mobility transistors (HEMTs).[1] AlGaN/GaN HEMTs are entering the commercial market and becoming established in the microwave power amplifier and power switching fields. Ensuring long term reliability and device lifetime are key requirements in many applications. Channel temperature is one of the main drivers of degradation in transistors,[2,3] in addition to other factors including electric fields.[4] Maximum power dissipation is often de-rated to keep the peak channel temperature within a safe working limit, ensuring reliability. Accurate channel temperature measurements are therefore crucial in this respect.[5,6] Moreover, channel temperature measurement aids the improvement of thermal design for low thermal resistance.[7,8] In this Letter, we report a Raman-based technique to directly access the temperature of the gate contact in AlGaN/GaN HEMTs, utilizing diamond microparticles capable of monitoring gate temperature on timescales as short as $10 \, \mu s$.

Joule self-heating in AlGaN/GaN HEMTs mainly occurs close to the AlGaN/GaN interface, within $0.5 \, \mu m$ of the drain-side edge of the gate foot.[9] There is a correspondingly localized peak channel temperature rise (ΔT_{peak}) at this location, as indicated in Fig. 1(a). A high temperature gradient exists, even on the sub-micron length-scale in AlGaN/GaN HEMTs. Measurements by conventional thermography methods, e.g., infrared thermography, are susceptible to spatial averaging.[10] Additionally, in pulse operation microsecond or sub-microsecond time resolution is required, depending on pulse length.

Raman micro-thermography is a versatile tool for thermal characterization of HEMTs; by monitoring the temperature-dependent shift in the frequencies of the Raman modes in semiconductor materials, it enables temperature measurements with $0.5 \, \mu m$ lateral spatial and 10 ns temporal resolution.[11] In AlGaN/GaN HEMTs this technique provides a volumetric average of temperature through the GaN layer (typical thickness $1-2 \, \mu m$), as illustrated in Fig. 1(a). However, even averaging on this length scale can lead to an underestimation of peak channel temperatures. Therefore, finite element method (FEM) thermal simulations are needed

to extrapolate the peak channel temperature from the Raman-measured temperature. In this case, the peak channel temperature accuracy could be influenced by uncertainties in FEM input parameters. In other device geometries, for example, field plates, areas with optical access to the underlying semiconductor are restricted; Raman thermography cannot be performed directly on metal surfaces. Optical access can be gained under the metal layers by measuring through transparent substrates,[12] although this is not possible, for example, in packaged devices.

In the standard procedure for peak channel temperature estimation, the measured GaN temperature is extrapolated using a thermal model whose input parameters include: substrate thermal conductivity, GaN layer thermal conductivity, and the thermal boundary resistance (TBR) associated with the nucleation layer. In order to ensure the highest peak channel temperature estimation accuracy, it is desirable to measure as close as possible to the gate contact. Based on device thermal modeling, the gate contact temperature is expected to be closer to the peak temperature than the volumetric GaN layer average. To extend Raman thermography to metal-covered areas, including the gate contact, we have developed a method using diamond micro-particles, deposited on the metal surface, acting as Raman "thermometers." Diamond microparticles are ideal for this purpose due to their high thermal conductivity, high Raman scattering efficiency, and transparency at the wavelength of the probing laser. This technique can be used not only for accurate steady-state or time-resolved surface temperature measurements in HEMTs but can also readily be applied to other device types or materials.

AlGaN/GaN HEMTs with $1.7 \, \mu m$ GaN and $25 \, nm$ AlGaN, with 3 nm GaN cap and 100 nm SiN passivation, on SiC substrates were studied. A $145 \, \mu m$ wide single-finger and a $100 \, \mu m$ wide two-finger device were measured. The single-finger device has a $10 \, \mu m$ source-drain gap, $0.75 \, \mu m$ long T-gate, and a $5 \, \mu m$ gate-drain gap. The two-finger device is a field-plate design, having a $5 \, \mu m$ source-drain spacing, $0.75 \, \mu m$ gate length, $3 \, \mu m$ gate-drain spacing, and a $20 \, \mu m$ gate pitch.

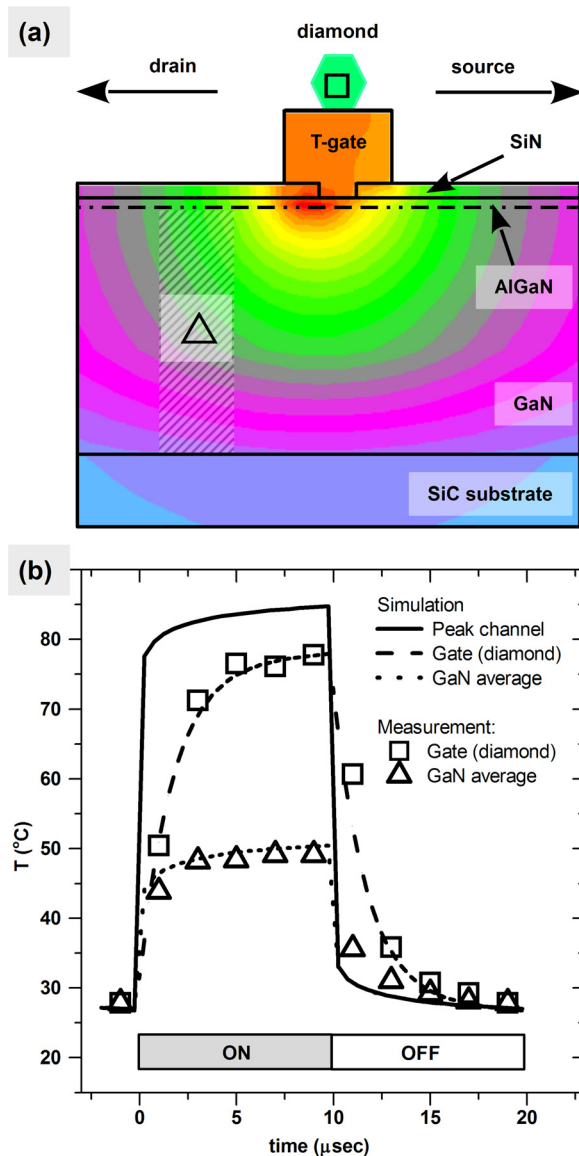The T-gated HEMT device and the field-plated HEMT device were both operated with a 50% duty cycle at 6 W/mm

FIG. 1. (a) Schematic cross-sectional structure of an AlGaN/GaN HEMT, with simulated temperature contours, showing the hot region at the gate edge and the volume where the temperature is measured by Raman thermography ($\triangle$). The diamond particle thermometer is shown on top of the gate ($\square$); (b) measured and simulated temperature transients of the GaN layer at 0.7 μm from the gate contact of an AlGaN/GaN HEMT, as indicated in (a), operated at 6 W/mm and a duty cycle of 50% and the temperature transients of the diamond particle on top of the gate. The simulated peak channel temperature transient is also shown.

and 7 W/mm peak power and 15 V and 10.6 V source-drain voltages, respectively.

Diamond particles with diameter of up to 1 μm were suspended in ethanol and deposited on the device surface using a pipette. A sufficiently high concentration of diamond particles was applied to ensure that particles were present on the gate (Figs. 1(a) and 3(a)).

A Renishaw InVia Raman system with 532 nm laser excitation and an acousto-optical modulator (AOM) were used to measure the temperature transients of GaN and the diamond particles with 0.5 μm lateral spatial resolution. Prior to the measurement, the temperature dependence of the Raman modes of several diamond particles had been investigated, and the obtained temperature coefficients were found to be identical for each particle and similar to those reported for

bulk diamond.[13] More details on Raman thermography and time-resolved Raman thermography can be found in Refs. [10] and [11]. The sample was mounted on a thermoelectric chuck and maintained at 25 °C. Sample position was controlled by a motorized XYZ translation stage with a 0.1 μm step size. A pattern recognition based auto-positioning routine was used to ensure that the probing laser remained focused and centered on the diamond particle under measurement. 3D thermal models were implemented in ANSYS® (Ref. [14]) for comparison to the measured device temperatures. In the thermal model of the T-gated device standard values for thermal conductivities of SiC, GaN, AlGaN, and SiN were used,[15–18] while the TBR represented by the AlN nucleation layer was fine-tuned within the expected range,[19] and the position and extension of the heater were adjusted to obtain the best fit for the measured GaN and diamond temperatures. The same parameters were then used to model the field-plated device where the TBR of the dielectric stack between the gate and the field plate was an adjustable parameter.

Figure 1(b) shows the measured and simulated temperature transients at a distance of 0.7 μm from the drain side edge of the gate ($\triangle$), corresponding to a volumetric average through the GaN layer. The measured and simulated temperature determined from the diamond particle ($\square$) located on top of the gate contact are also shown. The best agreement with the experimental data, illustrated in Fig. 1(b), was provided by a thermal model with TBR$_{AlN}$ of 0.6 m^{2}K/GW and a heater with a length of 0.375 μm, partially (0.125 μm) overlapping with the gate foot, similar to the previously reported results.[9] At the end of the 10 μs heating pulse, the measured gate temperature is about 10% lower than the simulated peak channel temperature—the 10% difference is caused by lateral heat spreading in the gate metal—whereas the measured GaN temperature is 41% lower. It has to be noted that a single-finger transistor is an extreme case, for a packaged multi-finger device the ΔT_{peak} to $\Delta T_{GaN\ average}$ ratio is smaller; consequently, the implications of minor differences in heater configuration are less significant. It is evident that diamond particle Raman thermography can provide good experimental basis for peak channel temperature estimation; moreover, applying diamond and standard Raman thermography in combination can also enable the refinement of FEM thermal models of the devices, as the gate temperature can serve as an additional boundary condition for the simulations. The use of this technique is particularly advantageous in the case of AlGaN/GaN HEMTs with field plates which typically cover parts of the GaN device surface, requiring standard Raman thermography to measure further away from the gate foot where heat is generated, as illustrated in Fig. 2(a), hence increasing the uncertainty of peak channel temperature estimation. Moreover, the dielectric layers and field plates covering the surface around the gate affect the thermal transport in the hot region. In this case, it is especially useful to obtain a further boundary condition for the simulations by measuring the temperature of the field plate. The temperature transient measured with the diamond particle thermometer on the source-connected field plate is displayed in Fig. 2(a) ($\square$), together with measured and simulated transients of the average temperature of the GaN layer in the field-plate-drain gap at a distance of 1.5 μm from
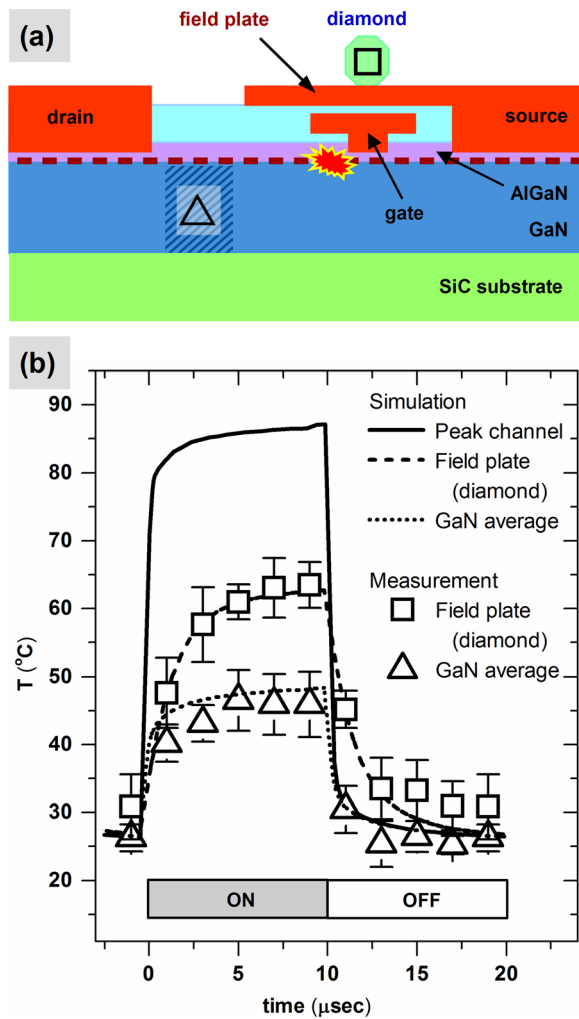
FIG. 2. (a) Schematic cross-sectional structure of the HEMT with source-terminated field plate, showing the corresponding positions of the temperature transients displayed in (b): diamond particle on the field plate (□) and the location of the standard Raman measurement (△); (b) measured and simulated temperature transients of the AlGaN/GaN HEMT operated at 7 W/mm with a 50% duty cycle: average temperature of the GaN layer in the field plate-drain gap (△), temperature of the diamond particle on the source-connected field plate over the gate (□), and the simulated peak channel temperature transient.

the gate edge (△). The simulated peak temperature is also shown. As expected, there is a larger difference between the simulated peak channel temperature and the temperature measured by diamond micro-thermometer than in the case of the T-gated device without field plate, which is due to the dielectric stack—SiN/SiO/SiON—between the field plate and the gate, which has a rather low thermal conductivity. By fitting the thermal simulation to the experimental data, we also determined a thermal resistance of the dielectric stack of 10.8 m^{2}K/GW. For the thermal management of such devices, this value can be important as large field plates, apart from spreading the electric field, also can act as heat spreaders, hence influencing the peak channel temperature.

One aspect that cannot be overlooked in any thermometric technique is a possible thermal contact resistance between the thermometer and the measured surface, e.g., due to rough surfaces; in our case, the diamond particle and the surface of the gate/field plate. Such thermal contact resistance could slow down the thermal response of the particle to the

changes in the temperature of the underlying surface. In the case of a large contact resistance and rapid changes the temperature of thermometer particle might be unable to follow the surface temperature; thereby, the measured temperature might differ from the instantaneous surface temperature. The possible effect of contact resistance has to be carefully examined in time-resolved measurements; in steady state measurements this issue is completely absent. Fig. 3(b) shows the temperature transient measured by the diamond thermometer placed on the T-gate—same data as in Fig. 1(b)—together with simulated transients of the gate surface temperature itself and the simulated transients of the diamond thermometer assuming different thermal contact resistances. The existence of a thermal resistance is apparent as the temporal evolution of the diamond particle's temperature is described by a somewhat larger thermal time constant than that is
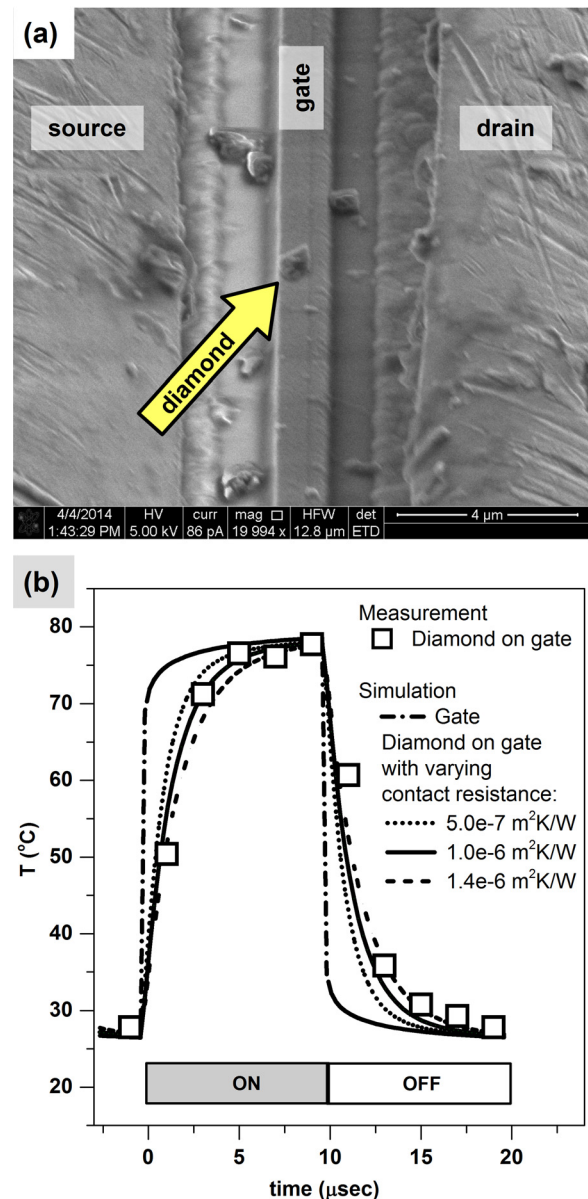

FIG. 3. (a) SEM image of a diamond particle on a source-connected field plate over the gate of an AlGaN/GaN HEMT; (b) measured temperature transient of a diamond particle located on T-gate (same as in Fig. 1(b)) and simulated temperature transients of the gate and the particle with different thermal contact resistances.

predicted by the simulation for the gate surface. The simulations also reveal that the contact resistance leaves the total temperature rise unaffected as long as time scales longer than 10 μs are considered, as the thermometer particle reaches thermal equilibrium after that period. At shorter time scales the delay in the temperature of the particle needs to be considered and the thermal contact resistance needs to be minimized.

In conclusion, diamond Raman micro-thermometers and their use for time-resolved gate contact temperature measurement in AlGaN/GaN HEMTs have been demonstrated, supplementing standard Raman thermography measurements. Temperature rise measured on the gate of a pulse-operated device with a diamond particle has been found to be close to the predicted peak channel temperature. The results indicate the technique's capability to provide good experimental basis for peak channel temperature estimations and to enable FEM thermal model refinement. The results obtained with the technique were in good agreement with earlier results from standard Raman thermography. Thermal behavior of a field-plated device has also been investigated, revealing that the top of the source-connected field plate was significantly lower than the peak channel temperature, yet higher than the temperature measured with standard Raman thermography. Furthermore, this generic technique can be used for steady-state or time-resolved temperature measurements with high spatial and temporal resolution in other material systems

[1]S. Y. Park, C. Floresca, U. Chowdhury, J. L. Jimenez, C. Lee, E. Beam, P. Saunier, T. Balistreri, and M. J. Kim, Microelectron. Reliab. **49**, 478 (2009).

[2]J.-B. Fonder, L. Chevalier, C. Genevois, O. Latry, C. Duperrier, F. Temcamani, and H. Maanane, Microelectron. Reliab. **52**, 2205 (2012).

[3]E. A. Douglas, C. Y. Chang, D. J. Cheney, B. P. Gila, C. F. Lo, L. Lu, R. Holzworth, P. Whiting, K. Jones, G. D. Via, J. Kim, S. Jang, F. Ren, and S. J. Pearton, Microelectron. Reliab. **51**, 207 (2011).

[4]M. Faqir, G. Verzellesi, G. Meneghesso, E. Zanoni, and F. Fantini, IEEE Trans. Electron Devices **55**, 1592 (2008).

[5]R. J. Trew, D. S. Green, and J. B. Shealy, IEEE Microwave Mag. **10**, 116 (2009).

[6]J. H. Leach and H. Morkoç, Proc. IEEE **98**, 1127 (2010).

[7]J. Pomeroy, M. Bernardoni, A. Sarua, A. Manoi, D. C. Dumka, D. M. Fanning, and M. Kuball, in *Proceedings of the IEEE Compound Semiconductor Integrated Circuit Symposium (CSICS)*, Monterey, CA, 13–16 October 2013, pp. 1–4.

[8]M. Faqir, T. Batten, T. Mrotzek, S. Knippscheer, M. Massiot, M. Buchta, H. Blanck, S. Rochette, O. Vendier, and M. Kuball, Microelectron. Reliab. **52**, 3022 (2012).

[9]S. Rajasingam, J. W. Pomeroy, M. Kuball, M. J. Uren, T. Martin, D. C. Herbert, K. P. Hilton, and R. S. Balmer, IEEE Electron Device Lett. **25**, 456 (2004).

[10]A. Sarua, H. Ji, M. Kuball, M. J. Uren, T. Martin, K. P. Hilton, and R. S. Balmer, IEEE Trans. Electron Devices **53**, 2438 (2006).

[11]G. J. Riedel, J. W. Pomeroy, K. P. Hilton, J. O. Maclean, D. J. Wallis, M. J. Uren, T. Martin, and M. Kuball, IEEE Electron Device Lett. **29**, 416 (2008).

[12]H. Ji, M. Kuball, A. Sarua, J. Das, W. Ruythooren, M. Germain, and G. Borghs, IEEE Trans. Electron Devices **53**, 2658 (2006).

[13]J. B. Cui, K. Amtmann, J. Ristein, and L. Ley, J. Appl. Phys. **83**, 7929 (1998).

[14]ANSYS®, Academic Research, Release 15.0.

[15]O. Nilsson, H. Mehling, R. Horn, J. Fricke, R. Hofmann, S. G. Muller, R. Eckstein, and D. Hofmann, High Temp. – High Pressures **29**, 73 (1997).

[16]J. Zou, D. Kotchetkov, A. A. Balandin, D. I. Florescu, and F. H. Pollak, J. Appl. Phys. **92**, 2534 (2002).

[17]W. Liu and A. A. Balandin, Appl. Phys. Lett. **85**, 5230 (2004).

[18]R. Beigelbeck, F. Kohl, F. Keplinger, J. Kuntner, and B. Jakoby, in *IEEE Sensors 2007 Conference*, Atlanta, GA, 28–31 October 2007, pp. 938–941.

[19]A. Manoi, J. W. Pomeroy, N. Killat, and M. Kuball, IEEE Electron Device Lett. **31**, 1395 (2010).